predicts that an average electron would gain only 190 eV of energy during the optical pulse. Thus assuming 30 eV are required to produce an ion pair, the ionization produced during the pulse would be many orders of magnitude below the experimentally observed value of 10^{13} ion pairs, determined by the charge collection experiments.

In the classical theories for breakdown at microwave frequencies, an electron can receive at most only the 10^{-3} eV of ordered oscillatory energy from the electric field in an electron-atom collision. However, at optical frequencies the absorption can become a quantum-dominated process, and the possibility exists that a large fraction of the photon energy can be transferred to an electron during a collision. The process of bremsstrahlung, photon radiation from electrons during an interaction with an atom or ion, is well known. The reverse process may also occur in which an electron gains energy by absorbing either the entire photon or some significant fraction of its energy during a collision with an atom.[5] It is felt that a process of this inverse bremsstrahlung type is the mechanism responsible for the breakdown at optical frequencies.

The authors would like to express their appreciation to Professor S. C. Brown of the Massachusetts Institute of Technology, Cambridge, Massachusetts for many helpful discussions and comments during the course of this work.

---

[1]F. J. McClung and R. W. Hellwarth, Proc. I.E.E.E. 51, 46 (1963).

[2]R. W. Terhune, Third International Symposium on Quantum Electronics, Paris, February 1963 (to be published).

[3]E. K. Damon and R. G. Tomlinson, Appl. Opt. 2, 546 (1963).

[4]S. C. Brown, Handbuch der Physik (Springer-Verlag, Berlin, 1956), pp. 531-574.

[5]H. A. Bethe and E. E. Salpeter, Quantum Mechanics of One- and Two-Electron Atoms (Springer-Verlag, Berlin, 1957), pp. 317-335.

SCATTERING OF RUBY-LASER BEAM BY GASES*

T. V. George, L. Slama,† M. Yokoyama,‡ and L. Goldstein
Gaseous Electronics Laboratory, University of Illinois, Urbana, Illinois
(Received 23 July 1963; revised manuscript received 11 October 1963)

The advent of the laser[1,2] has at last made it possible to made a detailed study of Rayleigh scattering.[3] Earlier measurements giving the right order of magnitude of the Rayleigh cross section were made at 90° in argon.[4]

With the development of monochromatic, coherent light sources and sensitive photodetectors, it is now possible to determine the angular distribution of the molecular scattering of light. A preliminary study of the divergence of the laser beam showed that the intensity of the laser light even at an angle of 80° was only reduced by a factor of 10^{-5} with respect to that of the forward beam.[5] This was found to be many orders of magnitude larger than the expected intensity of the light scattered from gas molecules. Thus it was necessary to design an optical system which would prevent this light from scattering off the walls of the apparatus. The schematic diagram of the system which reduced the spurious scattering to a tolerable level is shown in Fig. 1. The ruby-laser beam is focused at the center of the observation chamber by means of a long focal-length lens (focal length is 23.3 cm). The exit window is placed at the Brewster angle, and the observation chamber is shadowed from both the lens and window by two irises.

Observations are made in the horizontal plane. The scattered light is detected by photomultiplier No. 1 (RCA 7102), placed at the observation tubes which are located at every 15° around the scattering chamber. The light scattered from the exit window is detected by photomultiplier No. 2 (RCA 7102). Its output is used as the reference signal, since it is a measure of a quantity proportional to the intensity of the laser beam. Both photomultipliers are provided with appropriate interference filters.

The angular distribution of the scattered light observed in argon at atmospheric pressure and room temperature (296°K) is given in Fig. 2 and Fig. 3. Figure 2 shows the intensity variation for a horizontally polarized laser beam, and Fig. 3 shows the variation when the beam is vertically polarized.

The dashed line in Fig. 2 shows the $\cos^2\theta$ dependence predicted by Rayleigh's theory, fitted to the average experimental values obtained at

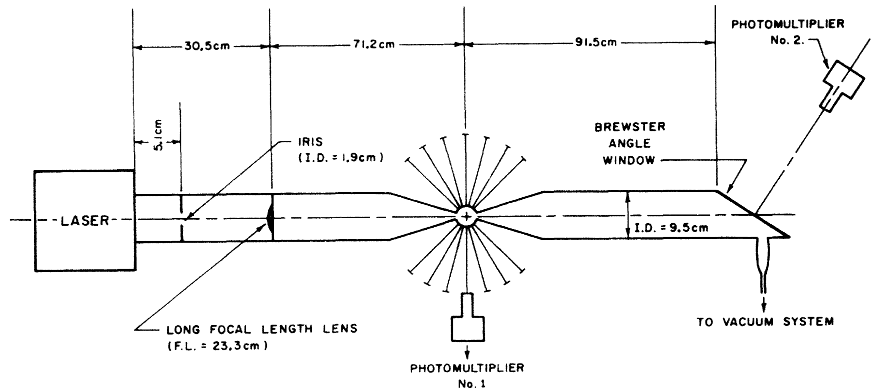

FIG. 1. Schematic diagram of experimental setup for the study of angular distribution of scattered-light intensity.

45° and 135°. Here θ is the angle between the direction of observation and the incident beam. Quantitative experimental studies of the polarization state of the incident beam as well as the field of view of the photomultiplier showed that the admixture of a vertically polarized radiation contributes 80% of the observed intensity at $\theta = 90°$, and the finite aperture of the detector accounts for the rest. The agreement between the experimental and theoretical curves is satisfactory. However, it is seen from Fig. 3 that, for the vertically polarized case, the intensity of the scattered light is not constant as a function of angle, as predicted by Rayleigh. The contribution of the horizontal component is less than 1.56% of that due to the vertical component at any angle θ. Hence the horizontal component alone does not account for the large deviation observed in the experiments. The theoretical curve showing the expected value of scattering is shown by the dashed line in Fig. 3. Completely similar results are obtained with

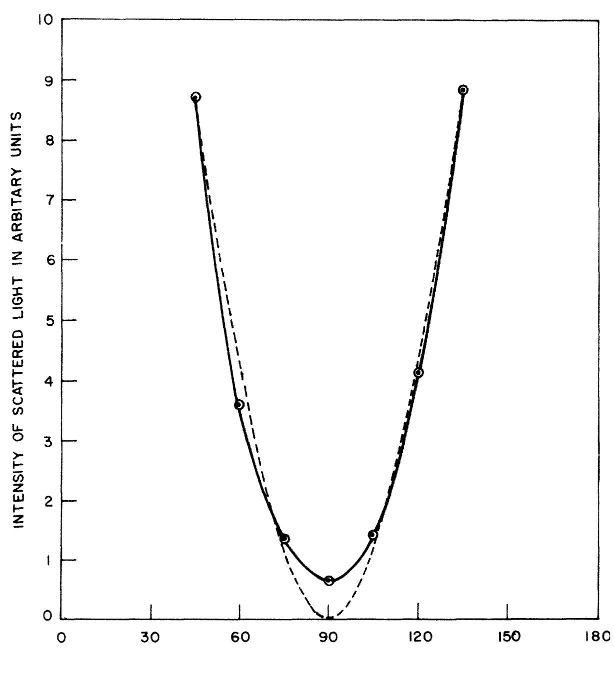

FIG. 2. Angular distribution of the intensity of scattered light for horizontally polarized incident beam in argon at atmospheric pressure.

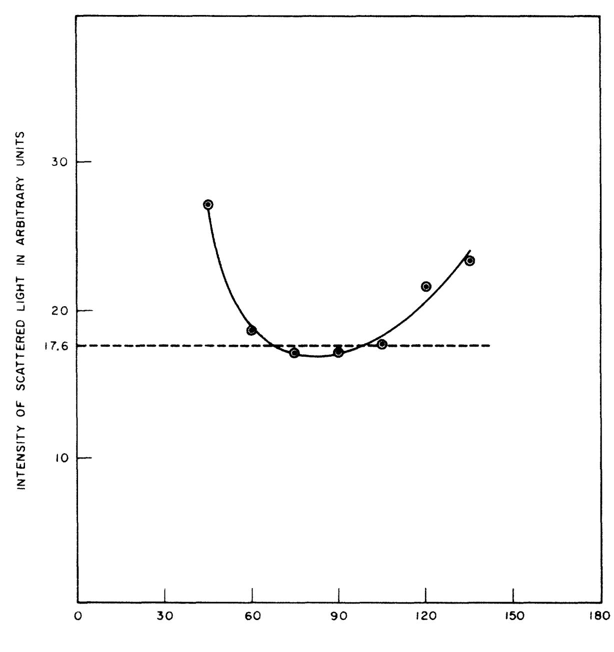

FIG. 3. Angular distribution of the intensity of scattered light for vertically polarized incident beam in argon at atmospheric pressure.

xenon.

Measurements of the intensity of scattered light were also made for various pressures in argon. The intensity of the scattered light was found to vary linearly with pressure at room temperature. The power of the incident laser beam was varied, and the ratio of the intensity of the scattered light to that of the incident beam was investigated. No substantial change in this ratio was observed for both monatomic and polyatomic gases, within the range of beam power levels used. All experiments were performed below the power level at which the gases would break down. The laser capacitors were charged to a maximum of twice the energy corresponding to the lasering threshold (307 joules).

Measurement of the differential scattering cross section for the polarization in the plane of observations at an angle of 60° with the forward direction of the laser beam was made in various gases at atmospheric pressure and room temperature (296°K). To calibrate photomultiplier No. 1, the laser beam was attenuated by a known thickness of copper sulfate solution and was detected by the same photomultiplier. By extrapolating the photomultiplier response curve to the limit as the thickness tended to zero, the intensity of the unattenuated beam was determined on the same scale by which the scattered light was measured. Precise measurements of the field of view of the photomultiplier and the solid angle subtended by the molecules at the photomultiplier were made at $\theta = 60°$, and the differential scattering cross section was determined.

According to the molecular theory of Rayleigh scattering in gases,[6] the differential scattering cross section is proportional to the square of the high-frequency polarizability of the scattering molecules. Through the Lorentz-Lorenz relation, the latter becomes proportional to $(n^2-1)^2$, where n is the refractive index of the gas for the radiation of wavelength under discussion. Table I gives the experimental and the calculated differential scattering cross sections at 60° with the direction of incidence. The differential scattering cross sections of monatomic gases seem to be about twice the theoretical cross-section values. Larger deviations are observed for molecular gases. In the monatomic gases, the ratios of the 60° differential scattering cross sections (Table II) are in close agreement with the theoretical ratios given by $[(n_1^2-1)/(n_2^2-1)]^2$ for gases 1 and 2.[7]

Table I. Differential scattering cross section for various gases.

Gas	Experimental values (10^{-28} cm^2)	Theoretical values (10^{-28} cm^2)
Ne	0.057	0.027
Ar	1.01	0.47
Xe	6.84	2.87
O_2	1.08	0.46
N_2	1.25	0.52
Air	1.23	0.50
CO_2	3.31	1.19
SF_6	7.28	...
C_3H_8	23.5	...

Table II. Ratios of the differential scattering cross sections for neon, argon, and xenon.

	Experimental values	Theoretical values
Ar/Ne	17.6	17.5
Xe/Ar	6.77	6.13
Xe/Ne	119	107

On the basis of the present results, (1) the angular distribution of the horizontally polarized radiation is verified to be proportional to $\cos^2\theta$ over the indicated angular range, (2) the vertically polarized radiation is not scattered isotropically as predicted by the theory, and (3) the differential scattering cross sections at $\theta = 60°$ are twice the calculated ones, with their ratios in close agreement with predictions.

A detailed account of this work will be submitted for publication.

Discussions with Dr. J. H. Cahn of the University of Illinois, Urbana, Illinois and Dr. L. Goldstein of the Los Alamos Scientific Laboratory, Los Alamos, New Mexico are gratefully acknowledged.

---

*This work was supported by U. S. Air Force Cambridge Research Laboratory and the U. S. Army Signal Corps.

†On leave of absence from Atomic Energy Commission, Saclay, France.

‡On leave of absence from Osaka University, Osaka, Japan.

[1]A. L. Schawlow and C. H. Townes, Phys. Rev. 112, 1940 (1958).

[2]T. H. Maiman, Phys. Rev. Letters 4, 564 (1960).

[3]Lord Rayleigh, Phil. Mag. 41, 107 (1871).

[4]J. Cabannes, Ann. Phys. (Paris) 15, 5 (1921).
[5]T. V. George, L. Slama, M. Yokoyama, and L. Goldstein (to be published).
[6]G. Placzek, Handbuch der Radiologie (Akademie Verlagsgesellschaft, Leipzig, Germany, 1934), Vol. VI, Part 2, pp. 205-274.
[7]G. A. Cook, Argon, Helium, and Rare Gases (Interscience Publishers, Inc., New York, 1961), Vol. 1.

THEORETICAL INTERPRETATION OF THE EQUATORIAL SPORADIC E LAYERS

K. Maeda and T. Tsuda
Department of Electronics, Kyoto University, Kyoto, Japan

and

H. Maeda
Geophysical Institute, Kyoto University, Kyoto, Japan
(Received 26 August 1963)

The purpose of this note is to make a theoretical explanation of the echo structure of the equatorial E_S. Up to this day, some authors have attempted to describe the formation of the equatorial E_S, e.g., from the viewpoint of two-stream plasma-wave instability,[1] etc.

Our theoretical basis is similar to that by Simon,[2] which is aimed at the instability analysis of weakly ionized plasmas. Particular modifications are done so as to make Simon's method applicable to the present ionospheric model. Let the rectangular coordinates be x, y, and z axes, which are in the geomagnetic N-S direction, W-E direction, and vertical upward direction, respectively. The background electron density (= positive ion density) is assumed to show a linear variation over a height range of L. The electrostatic field E_0 (>0) is applied in the W-E direction. Two equations of flux are introduced: one for the flux of electrons, the other for the flux of positive ions. Mobilities and diffusion coefficients across the magnetic field are supposed to be constant in this small height range. The charge density is put as follows:

$$n = n_0(z) + n_1(z)\exp(-i\omega t + ik_y y), \tag{1}$$

where k_y is the y component of the wave number $\vec{k}$, and the first and the second terms on the right-hand side are the unperturbed and the perturbed profiles of the charge density, respectively. We have another equation for E_0, which is similar to Eq. (1). n and E_0 are then required to satisfy the equations of motion. We neglect the higher order perturbation terms. Furthermore, $n_1(z)$ is assumed to vary as $N_1 \sin(\pi z/L)$ (N_1 = constant). We impose similar restrictions on the electrostatic field. Further approximations are made such that

$$|n_0^{-1}\langle dn_0/dz\rangle| \gg |E_0^{-1}\langle dE_0/dz\rangle|, \tag{2}$$

where

$$\left\langle\frac{dn_0}{dz}\right\rangle = \frac{1}{L}\int_0^L \frac{dn_0}{dz}\sin^2\left(\frac{\pi z}{L}\right)dz, \text{ etc.},$$

$$L \gg k_y^{-1}, \tag{3}$$

$$|n_0^{-1}\langle dn_0/dz\rangle| \gg 10 k_y^{-1}. \tag{4}$$

Thus the final condition for the growth or decay of the perturbation is given by

$$\mathrm{Re}(-i\omega) = \frac{(\omega_H\tau_c)^-(\mu_\perp^+)^2\mu_\perp^- E_0[(1/n_0)\langle dn_0/dz\rangle] - \mu_\perp^+(\mu_\perp^+ D_\perp^- + \mu_\perp^- D_\perp^+)k_y^2}{\{(\omega_H\tau_c)^+\mu_\perp^+ - (\omega_H\tau_c)^-\mu_\perp^-\}^2[(1/n_0)dn_0/dz]^2 k_y^{-2} + (\mu_\perp^+)^2}, \tag{5}$$

where superscripts "+" and "-" are attached to the quantities belonging to the positive ions and the electrons, respectively; "⊥" shows that the coefficient referred to is that perpendicular to the magnetic field; μ and D are the mobility and the diffusion coefficient, respectively; ω_H and τ_c are the gyration angular frequency and the mean collision time, respectively. From the above equation, in order that the instability grow [$\mathrm{Re}(-i\omega) > 0$], it is at least required that $E_0(n_0^{-1} \times \langle dn_0/dz\rangle) > 0$. When $E_0 > 0$, as is the case in day-